Physica A 388 (2009) 2278–2288

Contents lists available at ScienceDirect

Physica A

journal homepage: www.elsevier.com/locate/physa

A core-softened fluid model in disordered porous media. Grand canonical Monte Carlo simulation and integral equations

Orest Pizio [a,*,1], Hector Dominguez [b], Laszlo Pusztai [c], Stefan Sokołowski [d]

[a] Universidad Autonoma Metropolitana, Iztapalapa, Mexico, D.F., Mexico

[b] Instituto de Investigaciones en Materiales, UNAM, Coyoacan 04510, Mexico, D.F., Mexico

[c] Institute for Solid State Physics and Optics, Hungarian Academy of Sciences, Budapest, H-1121, Hungary

[d] Department for the Modelling of Physico-Chemical Processes, Maria Curie-Skłodowska University, 20031 Lublin, Poland

ARTICLE INFO

Article history:
Received 15 November 2008
Received in revised form 2 March 2009
Available online 18 March 2009

PACS:
61.20.Gy
61.20.Ja

Keywords:
Core-softened model
Disordered matrix
Adsorption
Integral equations
Computer simulation

ABSTRACT

We have studied the microscopic structure and thermodynamic properties of a core-softened fluid model in disordered matrices of Lennard-Jones particles by using grand canonical Monte Carlo simulation. The dependence of density on the applied chemical potential (adsorption isotherms), pair distribution functions, as well as the heat capacity in different matrices are discussed. The microscopic structure of the model in matrices changes with density similar to the bulk model. Thus one should expect that the structural anomaly persists at least in dilute matrices. The region of densities for the heat capacity anomaly shrinks with increasing matrix density. This behavior is also observed for the diffusion coefficient on density from independent molecular dynamics simulation. Theoretical results for the model have been obtained by using replica Ornstein–Zernike integral equations with hypernetted chain closure. Predictions of the theory generally are in good agreement with simulation data, except for the heat capacity on fluid density. However, possible anomalies of thermodynamic properties for the model in disordered matrices are not captured adequately by the present theory. It seems necessary to develop and apply more elaborated, thermodynamically self-consistent closures to capture these features.

1. Introduction

Understanding the behavior of simple and complex fluids in different porous media is of much importance for basic science and several applications [1–3]. In particular, many experimental and computer simulation studies have been performed to explore the microscopic structure, thermodynamic and dynamic properties of water in various environments [4–10]. However, the description of adsorption of even simple fluids in porous media is not a simple task in statistical mechanics. Several simplifications must be applied to explore these systems. Usually, it is assumed that the knowledge of thermodynamic behavior of a fluid in a single pore can be extrapolated to describe adsorption in more complex porous materials. Geometric characteristics of a single pore are considered as known. The slit-like, cylindrical and spherical pores are the most popular and useful models. Moreover, the fluid–wall interaction potential dependent solely on a single variable (distance of a particle from the surface) is commonly applied to provide understanding of the influence of the pore

* Corresponding author.
E-mail address: pizio@servidor.unam.mx (O. Pizio).

[1] On sabbatical leave from Instituto de Quimica de la UNAM.

0378-4371/$ – see front matter © 2009 Elsevier B.V. All rights reserved.
doi:10.1016/j.physa.2009.03.014

walls on the particles of adsorbed fluid. Under such assumptions several theoretical approaches have been developed to obtain the density profiles of species under confinement and calculate the adsorption isotherms. Integral equations have been widely used to solve the problem in the past. Nowadays, density functional approaches dominate area of the research, see e.g. Ref. [11] for a recent review.

On the other hand, precise description of adsorption phenomena for a wide set of systems with different levels of complexity can be reached by using computer simulation methods [2,3]. In particular, the grand canonical Monte Carlo (GCMC) simulation is one of the most useful approaches to obtain the adsorption isotherms. Moreover, the structure of pores and porous media can be described more adequately in simulations comparing to theoretical methods. Real porous materials are much more complicated than a collection of pores of well-defined geometry. Effects of geometric and energetic heterogeneity are intrinsically combined in the nature of adsorbents of practical importance.

One group of quite recent methodological developments [12,13] had focused on fluids adsorbed in disordered porous matrices or the so-called quenched–annealed fluids. The principal feature of these approaches is that a fluid and a disordered porous matrix are considered at the same footing. A matrix is considered as a collection of obstacles in a disordered fixed configuration mimicking an adsorbent. The partition function of the combined system consisting of a matrix and a fluid can be written in the replicated form and leads to the Helmholtz free energy averaged over possible matrix configurations. The free energy yields the adsorption isotherms and other properties of interest. A microscopic structure of adsorbed fluid can be obtained from replicated Ornstein–Zernike integral equations in close similarity to the methods for homogeneous bulk fluids. This type of modelling has been already used to describe a wide class of systems, see e.g. reviews [14,15]. Very recently the aforementioned methods have been extended to combine them with density functional approaches [16]. In parallel, computer simulations of such models have been performed to investigate the effects of matrix disorder on adsorption and test validity of the theoretical approaches [17–26]. Computer simulations permit to generate more sophisticated equilibrium and out of equilibrium matrix structures via specific algorithms and in some cases put them in correspondence to adsorbents of practical importance.

Undoubtedly, water is the most important substance for life, science and technology. However, many of its properties are not very well understood so far, even in the bulk, homogeneous systems. Several peculiarities or anomalies of the properties of water in liquid and solid states have been reported and discussed in detail [27–29]. A large set of studies concerning the relation between the structural and dynamic anomalies and their connection with thermodynamic properties has appeared recently, see e.g. Refs. [30,31] for comprehensive reviews. Some other tetrahedrally bonded molecular liquids, besides water, also exhibit thermodynamic and dynamic anomalies [32,33]. Several models for intermolecular interaction potentials have been proposed in order to describe adequately these types of systems. In the particular case of water, it has been shown, by using molecular dynamics simulations for the SPC-E model, that the structurally anomalous region of states englobes the diffusion and density anomaly region [29,34]. Much simpler isotropic model potentials have been developed to understand the physics behind liquid state anomalies. In particular, the core-softened potentials are characterized by a repulsive core and an additional region of softer repulsion where the slope dramatically changes with respect to the core. This special region can have a form of a repulsive shoulder or a ramp [35,36]. A model ramplike interaction with continuous potential and force has been proposed and studied recently [37–39]. The authors of these works have used molecular dynamics simulation and integral equations theory to demonstrate that the model exhibits structural, density and dynamic anomalies. Therefore, it seems interesting to employ the model to other more complex systems, in particular to the problem of adsorption in pores and in porous media.

In the present work, we would like to investigate the microscopic structure and thermodynamic properties of the fluid model with soft-core interaction adsorbed in disordered porous media. Our principal interest is to explore how anomalies observed in the bulk are affected and if they persist in the fluid adsorbed in disordered porous matrices.

2. The model and computational method

The system we would like to consider consists of two subsystems, namely the porous medium and the fluid penetrating it. The porous structure is entirely independent on the afterwards process, during which the fluid particles fill the medium. On the other hand, the fluid subsystem essentially depends on the properties of the porous medium. Such a theoretical setup is in accordance with experimental studies, if one excludes swelling phenomena or matrix rupture.

At the first stage, the disordered porous material, called the matrix in what follows, has been generated by considering N_m, ($N_m = 10^3$) particles in a cubic box with the edge L. Periodic boundary conditions have been applied, as common. The potential energy of the matrix subsystem is a sum of pairwise Lennard-Jones (LJ) interaction potentials,

$$u_{mm}(r) = 4\varepsilon_m[(\sigma_m/r)^{12} - (\sigma_m/r)^6], \tag{1}$$

where σ_m and ε_m denote the diameter of matrix species and the interaction energy, respectively.

In order to perform adsorption studies via GCMC simulation, we use equilibrium homogeneous matrices at different densities, $\rho_m^* = 0.1$, 0.2 and 0.3 ($\rho_m^* = N_m(\sigma_m/L)^3$), all prepared at $T_m^* = 1.5$ ($T_m^* = k_B T_m/\varepsilon_m$). The configurations of particles in each matrix have been taken from our recent molecular dynamics study [40] and we refer the reader to this work for technical details to avoid unnecessary repetition.

The fluid subsystem consists of particles that interact via isotropic core-softened potential,

$$u_{ff}(r) = 4\varepsilon_f[(\sigma_f/r)^{12} - (\sigma_f/r)^6] + a\varepsilon_f \exp\left[-\left(\frac{r-r_0}{\sigma_f}\right)^2\right], \tag{2}$$

where σ_f and ε_f denote the diameter of particles and the interaction energy, respectively. The values of other parameters are taken according to the study of the bulk model [37,38], $a = 5$, $r_0/\sigma_f = 0.7$. One must have in mind that there exists a delicate balance between the LJ contribution and the Gaussian term in the potential above, even a slight change of parameters can alter thermodynamic properties of the model and "destroy" anomalies of the properties one is seeking for.

The interaction between fluid and matrix particles is chosen as the LJ potential in close similarity to Eq. (1), however with appropriate parameters,

$$u_{fm}(r) = 4\varepsilon_{fm}[(\sigma_{fm}/r)^{12} - (\sigma_{fm}/r)^6], \tag{3}$$

where the Lorentz–Berthelot mixing rules are applied $\sigma_{fm} = (\sigma_f + \sigma_m)/2$ and $\varepsilon_{fm} = (\varepsilon_f\varepsilon_m)^{1/2}$. Moreover, to reduce the number of parameters of the model to a minimum, in this work we restrict ourselves to the case of equal diameters of matrix and fluid particles, $\sigma_m = \sigma_f = \sigma$. Without loss of generality we choose the length unit, $\sigma = 1.0$.

The GCMC simulation of the fluid subsystem in the given matrix is performed according to standard routine [41]. We studied the systems in a cubic box determined by previous matrix simulation of the size $L \times L \times L$ with periodic boundary conditions in all directions. The equilibrium states were usually reached after 2×10^5 steps per atom. The averages were calculated over the next 7×10^5 steps. To avoid correlations between subsequently generated states, the sampling of averages was carried out at the intervals of 10^3 steps. The output of simulations is given in terms of the dependence of fluid density on the applied chemical potential at a given temperature T_f^* ($T_f^* = k_BT_f/\varepsilon_f$, ε_f is chosen as the energy unit in what follows).

We have also calculated the heat capacity from the fluctuations of the Hamiltonian, $\mathcal{H} = U - N_f\mu_f$, where U is the potential energy of the system involving N_f fluid and N_m matrix particles. The configurational heat capacity per unit volume is then given by

$$c_v = [\langle\mathcal{H}^2\rangle - \langle\mathcal{H}\rangle^2]/(Vk_BT_f^2). \tag{4}$$

Besides, the pair distribution functions, $g_{ff}(r)$ and $g_{fm}(r)$, are obtained as common. All the properties have been obtained in two copies of matrices prepared at the same conditions during independent runs. However, we have confirmed that similar to previous studies of the models of the same type as we consider, such an averaging does not alter the structural and thermodynamic properties significantly.

Let us proceed now to the theoretical background. Our approach is similar to that previously reported in several applications [42–44]. Therefore, we omit some details. The matrix structure in terms of the pair distribution function $g_{mm}(r)$ ($g_{mm}(r) = 1 + h_{mm}(r)$) comes from the solution of common Ornstein–Zernike integral equation

$$h_{mm}(r_{12}) - c_{mm}(r_{12}) = \rho_m \int \mathrm{d}\mathbf{r}_3 c_{mm}(r_{13})h_{mm}(r_{32}), \tag{5}$$

with the hypernetted chain closure

$$1 + h_{mm}(r) = \exp[-u_{mm}(r)/k_BT_m]\exp[h_{mm}(r) - c_{mm}(r)], \tag{6}$$

where $c_{mm}(r)$ is the direct correlation function. On the other hand, the fluid–matrix and fluid–fluid distribution functions are obtained from the replicated form of the Ornstein–Zernike equations

$$h_{fm}(r_{12}) - c_{fm}(r_{12}) = \rho_m \int \mathrm{d}\mathbf{r}_3 c_{fm}(r_{13})h_{mm}(r_{32}) + \rho_f \int \mathrm{d}\mathbf{r}_3[c_{ff}(r_{13}) - c_{ff}^{bl}(r_{13})]h_{fm}(r_{32}), \tag{7}$$

$$h_{ff}(r_{12}) - c_{ff}(r_{12}) = \rho_m \int \mathrm{d}\mathbf{r}_3 c_{fm}(r_{13})h_{fm}(r_{32}) + \rho_f \int \mathrm{d}\mathbf{r}_3 c_{ff}(r_{13})h_{ff}(r_{32}) - \rho_f \int \mathrm{d}\mathbf{r}_3 c_{ff}^{bl}(r_{13})h_{ff}^{bl}(r_{32}), \tag{8}$$

$$\begin{aligned} h_{ff}^{bl}(r_{12}) - c_{ff}^{bl}(r_{12}) \;=\; & \rho_m \int \mathrm{d}\mathbf{r}_3 c_{fm}(r_{13})h_{fm}(r_{32}) + \rho_f \int \mathrm{d}\mathbf{r}_3 c_{ff}(r_{13})h_{ff}^{bl}(r_{32}) \\ & + \rho_f \int \mathrm{d}\mathbf{r}_3 c_{ff}^{bl}(r_{13})h_{ff}(r_{32}) - 2\rho_f \int \mathrm{d}\mathbf{r}_3 c_{ff}^{bl}(r_{13})h_{ff}^{bl}(r_{32}), \end{aligned} \tag{9}$$

with the closures

$$1 + h_{fm}(r) = \exp[-u_{fm}(r)/k_BT_f]\exp[h_{fm}(r) - c_{fm}(r)], \tag{10}$$

$$1 + h_{ff}(r) = \exp[-u_{ff}(r)/k_BT_f]\exp[h_{ff}(r) - c_{ff}(r)], \tag{11}$$

$$1 + h_{ff}^{bl}(r) = \exp[h_{ff}^{bl}(r) - c_{ff}^{bl}(r)], \tag{12}$$

where h_{ff}^{bl} and c_{ff}^{bl} are the blocking pair correlation function and the blocking direct correlation function, respectively.

The chemical potential of fluid species in disordered media in this formalism can be obtained straightforwardly from the expression already explored in several works, see e.g. Ref. [45],

$$\mu_f/k_BT_f = -\rho_m \int \mathrm{d}\mathbf{r} c_{fm}(r) - \rho_f \int \mathrm{d}\mathbf{r}[c_{ff}(r) - c_{ff}^{bl}(r)] + \frac{1}{2}\rho_m \int \mathrm{d}\mathbf{r} h_{fm}(r)(h_{fm}(r) - c_{fm}(r)) + \frac{1}{2}\rho_f \int \mathrm{d}\mathbf{r} h_{ff}(r)(h_{ff}(r) - c_{ff}(r)) - \frac{1}{2}\rho_f \int \mathrm{d}\mathbf{r} h_{ff}^{bl}(r)(h_{ff}^{bl}(r) - c_{ff}^{bl}(r)). \quad (13)$$

The internal energy per fluid particle is well defined for quenched–annealed fluids. It reads

$$\frac{1}{N_f}U_{ex} = \frac{1}{2}\rho_f \int \mathrm{d}\mathbf{r} g_{ff}(r) u_{ff}(r) + \rho_m \int \mathrm{d}\mathbf{r} g_{fm}(r) u_{fm}(r). \quad (14)$$

Then, it is straightforward to obtain heat capacity as the derivative of energy over temperature. In the ROZ/HNC the reduced heat capacity per fluid particle can be written in close similarity to common fluid mixture in the bulk [46].

$$\bar{c_v} = 2\pi\rho_f \int dr r^2 g_{ff}(r)\beta_f u_{ff}(r)\left[\beta_f u_{ff}(r) - \beta_f \frac{\partial\omega_{ff}(r)}{\partial\beta_f}\right] + 4\pi\rho_m \int dr r^2 g_{fm}(r)\beta_f u_{fm}(r)\left[\beta_f u_{fm}(r) - \beta_f \frac{\partial\omega_{fm}(r)}{\partial\beta_f}\right] \quad (15)$$

where $\omega_{ab} = h_{ab}(r) - c_{ab}(r) + B_{ab}(r)$ $(a, b = f, m)$, $\beta_f = (k_BT_f)^{-1}$

$$\bar{c_v} = \frac{c_v}{N_f k_B} - \frac{3}{2}. \quad (16)$$

However, the bridge functions are vanishing, $B_{ab}(r) = 0$, in the framework of the ROZ/HNC approximation employed in the present work. Note that the heat capacities from Eqs. (4) and (15) differ by the normalization constant (while the former is calculated in the grand canonical ensemble simulation per unit volume, the latter is normalized by the number of particles). Thus, we have renormalized theoretical results to provide comparison with simulation data in what follows. Let us proceed now to the description of the results. A detailed comparison of each of the properties discussed above coming from integral equations method and GCMC computer simulations is provided below.

3. Results and discussion

In the three panels of Fig. 1 we present the dependence of the fluid density on the chemical potential ($\mu^* = \mu_f/\varepsilon_f$) for the bulk model and in the three matrices that differ by density from the GCMC simulations. The data shown in part a of this figure have been obtained at rather high fluid temperature, $T_f^* = 1.0$. It appears that the adsorbed fluid density in matrices at a low ($\rho_m^* = 0.1$) and an intermediate ($\rho_m^* = 0.3$) density is higher than that for the bulk fluid at the same chemical potential in the entire range of the chemical potential studied. It seems that the number of adsorbing obstacles plays a dominant role in this effect, because the adsorbed density is higher in the case $\rho_m^* = 0.3$ comparing to $\rho_m^* = 0.1$. If the matrix density is increased further, i.e. $\rho_m^* = 0.5$, one can see that the excluded volume effect of the matrix overcomes the effect due to the increasing number of adsorbing obstacles, the corresponding curve crosses adsorption isotherms for a fluid in less dense matrices and next crosses the relevant projection of the equation of state for the bulk model. It is worth mentioning that the shape of curves is almost linear.

A set of results similar to that in Fig. 1a is shown in Fig. 1b. However, these data are obtained at a lower temperature, $T_f^* = 0.5$. The features discussed with respect to the data in Fig. 1a preserve. However, it is important to mention that the curve corresponding to the matrix $\rho_m^* = 0.5$ crosses the bulk curve at fluid density $\rho_f^* \simeq 0.19$, in contrast to $\rho_f^* \simeq 0.13$ in Fig. 1a ($\rho_f^* = \rho_f\sigma_f^3$). This behavior can be attributed to stronger fluid–fluid correlations as a result of lower T_f^* and slightly stronger fluid–matrix attraction (recall that we apply combination rules for the energy of fluid–matrix interaction). Finally, in Fig. 1c we present the adsorption isotherms at a quite low temperature, $T_f^* = 0.2$, for the bulk system and in the three matrices. Again, it appears that for a system with higher matrix density, adsorption is higher in comparison to lower matrix density. To conclude our explanation of the results of Fig. 1, we would like to note that the trends of behavior of adsorption isotherms can be explained not only by matrix density (density of adsorbing centers). Specific behavior of adsorption for the system in question in comparison to, for example, a hard sphere fluid, arise due to the softness of interaction between fluid species. Therefore, even formally a quite dense matrix can accommodate a reasonably high number of fluid particles. These two factors, matrix density and softness of fluid–fluid potential, besides the temperature of adsorption, determine the behavior of relevant isotherms.

In Fig. 2 we present the adsorption isotherms from the GCMC simulation and theoretical curves coming from ROZ/HNC approximation. The curves obtained by the same methods for the bulk fluid are given also for the sake of comparison. Nominal matrix density is quite high $\rho_m^* = 0.3$ but the temperatures of observation are very different. In the case of a high temperature, $T_f^* = 0.5$ (Fig. 2a), the theory describes adsorption perfectly well. The isotherm is almost linear with the exception of low values of the chemical potential. However, at much lower temperature, $T_f^* = 0.1$ (Fig. 2b), we observe discrepancy between the theory and simulation in the range of densities between 0.1 and 0.18, approximately. The largest

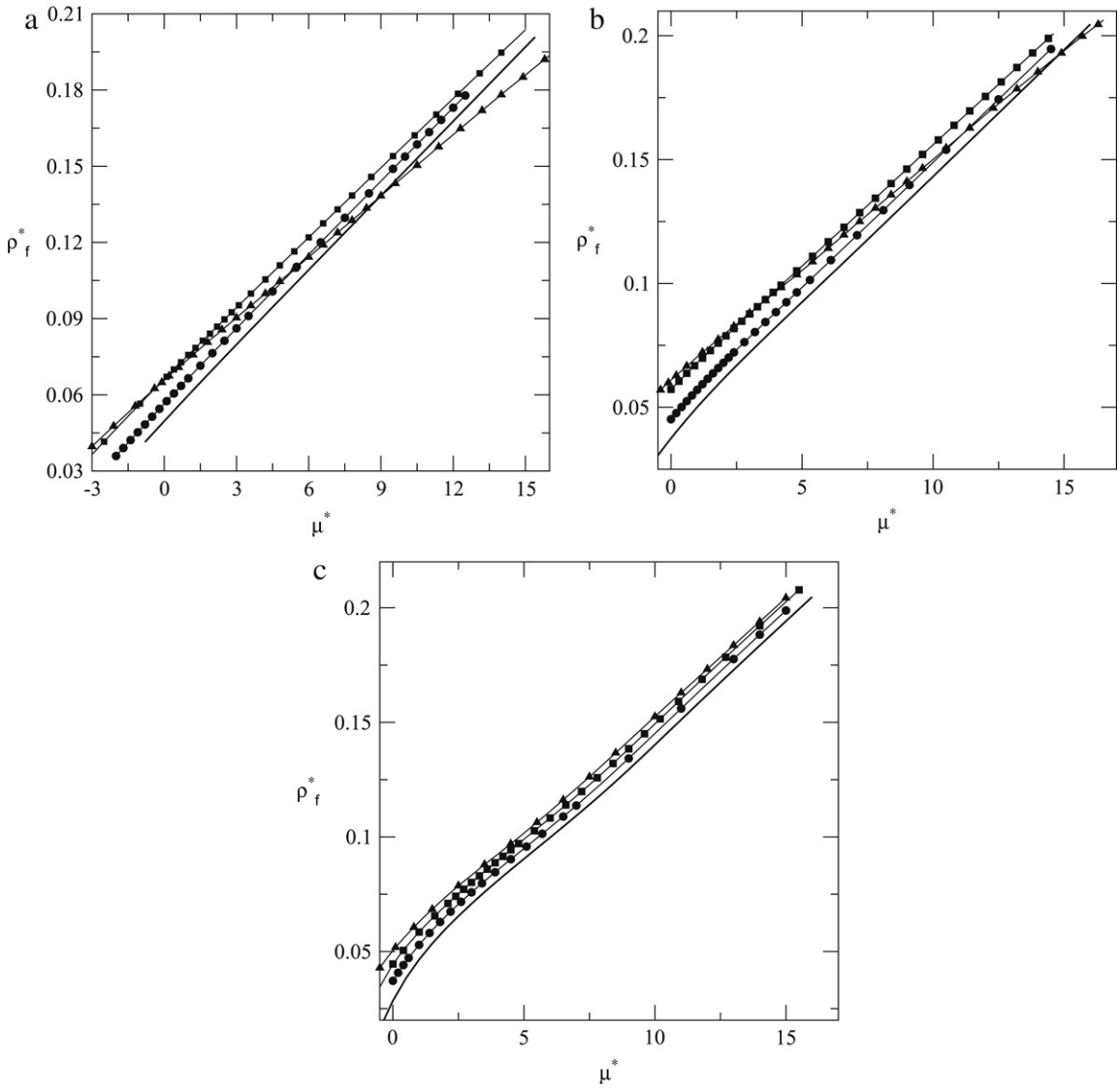

Fig. 1. Part a: Equation of state for the bulk core-softened model fluid and confined in matrices of different densities in μ^*- ρ^*_f plane. The solid line, circles, squares and triangles are the GCMC simulation points for the bulk fluid, the fluid in the matrix at $\rho^*_m = 0.1$, $\rho^*_m = 0.3$ and $\rho^*_m = 0.5$, respectively, $T^*_m = 1.5$. In all cases $T^*_f = 1.0$. The lines are given in all panels of this figure for better visualization. Part b: The same as in part a but at lower fluid temperature, $T^*_f = 0.5$. The nomenclature is like in part a. Part c: The same as in parts a and b but at $T^*_f = 0.2$. The solid line, circles, squares and triangles are the GCMC simulation data corresponding to the bulk fluid, the fluid in the matrix at $\rho^*_m = 0.1$, $\rho^*_m = 0.2$ and $\rho^*_m = 0.3$, respectively.

disagreement is at densities between 0.11 and 0.16. This is precisely the region of densities at which the model in the bulk exhibits anomaly [37–39]. The GCMC data show that the inclination of this isotherm, $T^*_f = 0.1$, changes or in other words the derivative $\mathrm{d}\rho_f/\mathrm{d}\mu_f$ has a maximum in the interval of fluid densities between 0.12 and 0.14. This type of behavior has been discussed by us very recently using computer simulation data for the bulk model in a separate work and is the only peculiarity observed on the dependence of adsorbed density on chemical potential [47]. The ROZ/HNC approach does not capture such a trend in the limiting case of the bulk model (i.e. matrix density tends to zero) as well as for adsorbed fluid. We would like to get knowledge about the reasons of observed discrepancy between theory and simulations and therefore perform detailed comparison of the distribution functions form the ROZ/HNC approach and computer simulations in a wide range of thermodynamic states.

First, in Fig. 3 we compare the fluid–fluid and fluid–matrix distribution functions at high temperature, $T^*_f = 0.5$. The theory is very good in describing both functions for a wide range of fluid densities. The only small drawback is in the description of the first growing maximum at $r \simeq 1.0$ at intermediate density around $\rho^*_f = 0.101$ (Fig. 3b). The principal maximum of the function $g_{ff}(r)$ at $r \simeq 2.2$ is described quite well. Also, the function g_{fm} from the integral equations theory agrees well with simulations. The evolution of the fluid–fluid distribution function with augmenting density

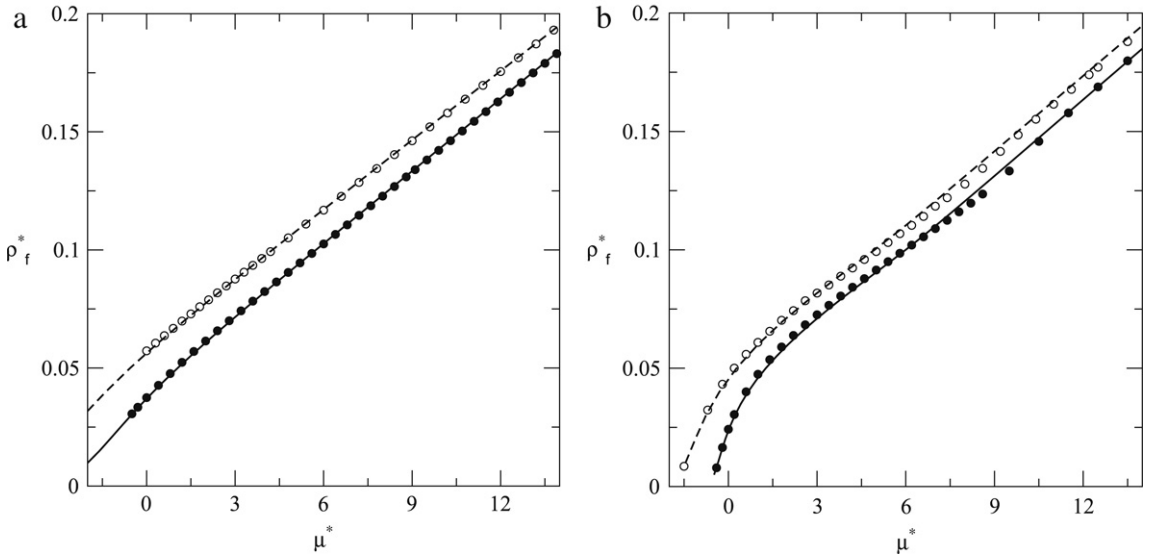

Fig. 2. The GCMC simulation data (hollow circles) and the results from the ROZ/HNC approach (dashed lines) for adsorption isotherms at $T_f^* = 0.5$ (part a) and at $T_f^* = 0.1$ (part b) in the matrix at $T_m^* = 1.5$, $\rho_m^* = 0.3$. The GCMC data (filled circles) and HNC isotherms $\rho_f^* - \mu^*$ (solid lines) for the bulk core-softened fluid are given in each panel for the sake of comparison.

(chemical potential) is quite similar to the one observed for bulk model. At low fluid density the principal maximum of $g_{ff}(r)$ describing neighbors of a given fluid particle is located at $r \simeq 2.2$. The number of neighbors in this coordination shell decreases in the expense of increasing coordination number corresponding to the maximum at $r \simeq 1.0$. It is the result of softness of the repulsive fluid–fluid interaction when the chemical potential grows up. The principal maximum for the fluid–matrix distribution function grows simultaneously but weakly. Moreover, the second shell of fluid particles around a given matrix particle is weakly pronounced. It can be said that the mean force fluid–fluid potential is in fact quite weakly influenced by the presence of matrix species at these conditions.

A set of results concerning pair distribution functions in the same matrix but at lower temperature of observation, $T_f^* = 0.1$, is given in Fig. 4. At this temperature the correlations between all the species are stronger, this can be seen comparing the heights of the maxima for the pair distribution functions with previously considered case of a higher temperature. The ROZ/HNC approximation provides a very good description of the fluid–matrix correlations at all densities studied. The fluid–fluid distribution function is well described at low fluid density and provides a qualitatively correct picture at high fluid density. However, the intermediate densities are not described adequately. In particular, the HNC overestimates the first maximum at $r \simeq 1.0$ and trends to its growth (Fig. 4c), also the second maximum at $r \simeq 2.2$ is overestimated at intermediate and high density (Fig. 4d, e). This is precisely the region at which one should expect the density anomaly for the model in question.

It is important to mention that at low temperature studied, strong correlations between fluid species can be implicitly seen in the formation of shells around a given matrix particle. The first and the second coordination shell of a matrix particle are well defined, in contrast to our observations at a higher temperature $T_f^* = 0.5$, cf. Fig. 3. On the other hand, at reasonably high adsorbed fluid density (Fig. 4d, e) the potential of the mean force between fluid species is influenced by the presence of matrix particles, as can be deduced from the specific shape of the $g_{ff}(r)$ at $r \simeq 3.0$. One can use the ROZ/HNC approximation to describe overall trends of adsorption and microscopic structure of a fluid in the matrix with reasonable success but finer effects, such as possible density anomaly, are not captured by this closure. Thus, one needs to resort to more elaborated thermodynamically self-consistent closures in the spirit of Rogers–Young approximation or resort to computer simulations data.

Our previous considerations have been concerned with simulation data and theoretical results that involve solely integration of the pair distribution functions at a given thermodynamic state. One of the most stringent tests of the accuracy of integral equation results is provided if one attempts the calculation of heat capacity. In the course of performing the GCMC simulation we have calculated the fluctuations of the Hamiltonian of the system, cf. Eq. (4). On the other hand, reduced heat capacity can be obtained in the framework of theoretical approaches according to Eq. (15). This expression involves temperature derivative of the correlation functions, and in general of the bridge function. In many previous applications the principal attention has been in parametrization of the density dependence of the bridge function. However, the temperature dependence of this function is not of less importance especially for the fluids exhibiting thermodynamic anomalies.

Heat capacities (normalized by the volume, $c_v^* = \bar{c_v}\rho_f^*$, from simulations and theory) are given in Fig. 5. We observe that the heat capacity for the bulk model according to GCMC data exhibit weak tendency to anomalous behavior even at rather high temperature, $T_f^* = 0.5$ (Fig. 5a). Namely the heat capacity slightly decreases with decreasing density in the interval

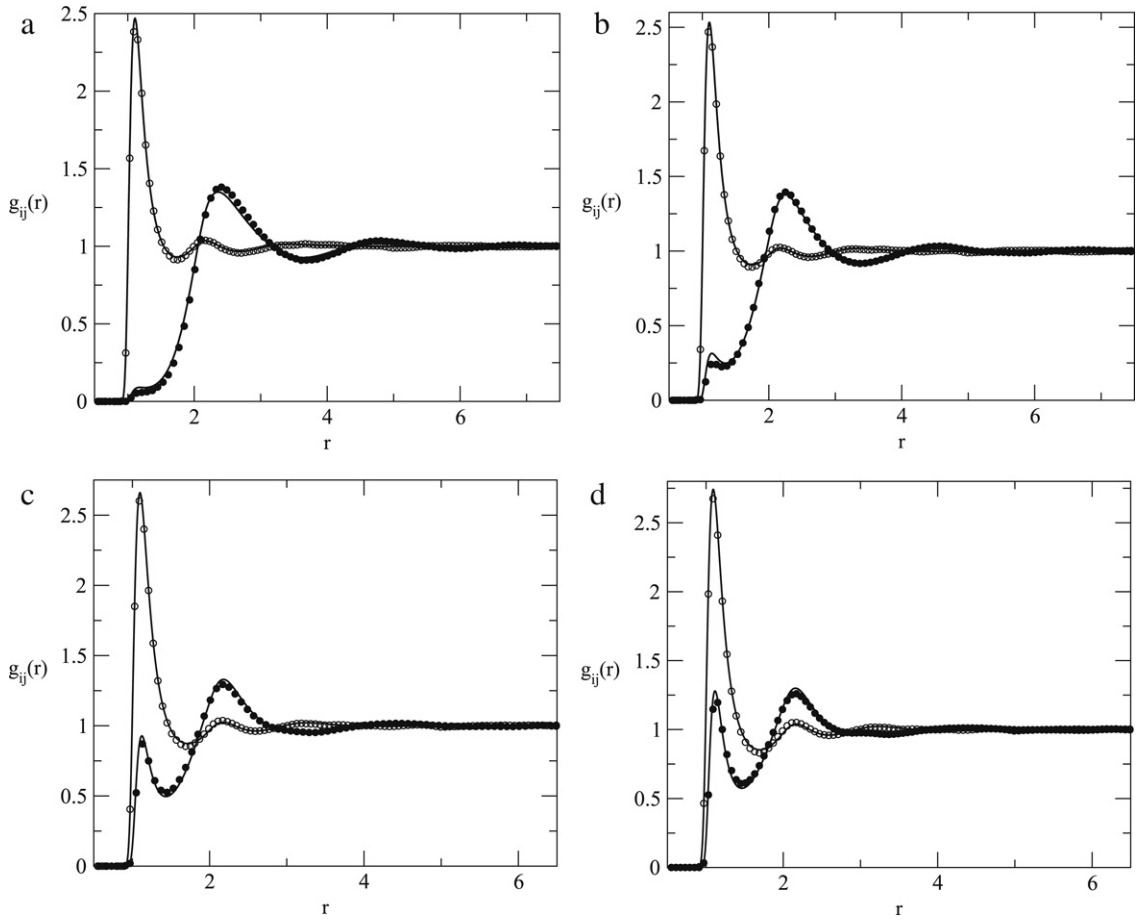

Fig. 3. A comparison of the fluid–matrix and fluid–fluid pair distribution functions from the ROZ/HNC approximation (solid lines) and GCMC simulation data (hollow circles – fluid–matrix, filled circles – fluid–fluid) for the system at $\rho_m^* = 0.3$, $T_m^* = 1.5$, at $T_f^* = 0.5$. Parts a, b, c and d correspond to $\mu^* = 1.2$, $\mu^* = 4.4$, $\mu^* = 10.4$ and $\mu^* = 14.4$, respectively. The adsorbed fluid densities approximately are: 0.07, 0.101, 0.16 and 0.20, respectively.

from $\rho_f \simeq 0.12$ till $\rho_f \simeq 0.15$. However, the same curves in two matrices considered, $\rho_m^* = 0.1$ and $\rho_m^* = 0.3$ do not show anomaly at all, the heat capacity grows with increasing fluid density at $T_f^* = 0.5$. The ROZ/HNC approach describes growth of the heat capacity qualitatively correct only in the region of low adsorbed densities. At higher fluid density the theory fails to follow simulation data. If the temperature of observation is lower, $T_f^* = 0.2$ (Fig. 5b), computer simulations show that the anomaly of heat capacity exists in the bulk in almost the same density range. The anomaly preserves for low density matrix $\rho_m^* = 0.1$ and to a smaller extent for the fluid in high density matrix $\rho_m^* = 0.3$. However, it seems that the density interval in which the heat capacity decreases shrinks and apparently will disappear at a higher matrix density at the temperature considered. One can conclude that the anomaly shrinks and eventually disappears when the contribution of the fluid–matrix interactions into the internal energy and into its temperature derivative increases and becomes more important than the relevant contributions from the fluid–fluid correlations. Theoretical predictions are not satisfactory at this temperature, or in other words the HNC approximation does not yield correct temperature derivative of the pair and direct correlation functions.

It is well established for the bulk model that peculiarities of the microscopic structure and thermodynamic anomalies on the one hand and the dynamic anomalies on the other are intrinsically related. A contribution coming from pair correlations to entropy has been introduced as a quantitative measure of the structural anomalies [48]. It looks possible but is not straightforward to extend this type of measure to quenched–annealed fluids. Thus we postpone relevant investigation to future studies. However, we have observed that the peculiarities of the behavior of adsorption isotherms occur approximately in the same density interval where the heat capacity shows anomaly. It is of interest to explore if and how these trends of behavior relate to dynamic properties.

Recently, we have reported a set of simulation data for the diffusion coefficient of the core-softened model in the bulk and under confinement in disordered matrices obtained by using molecular dynamics [40]. We refer the reader to this publication for all methodological and technical details. Here we just use the data obtained by us previously and some additional results by the same method to get additional insight into the relation between thermodynamic and dynamic anomalies for the model in question. In particular, the dependence of the diffusion coefficient of core-softened fluid model

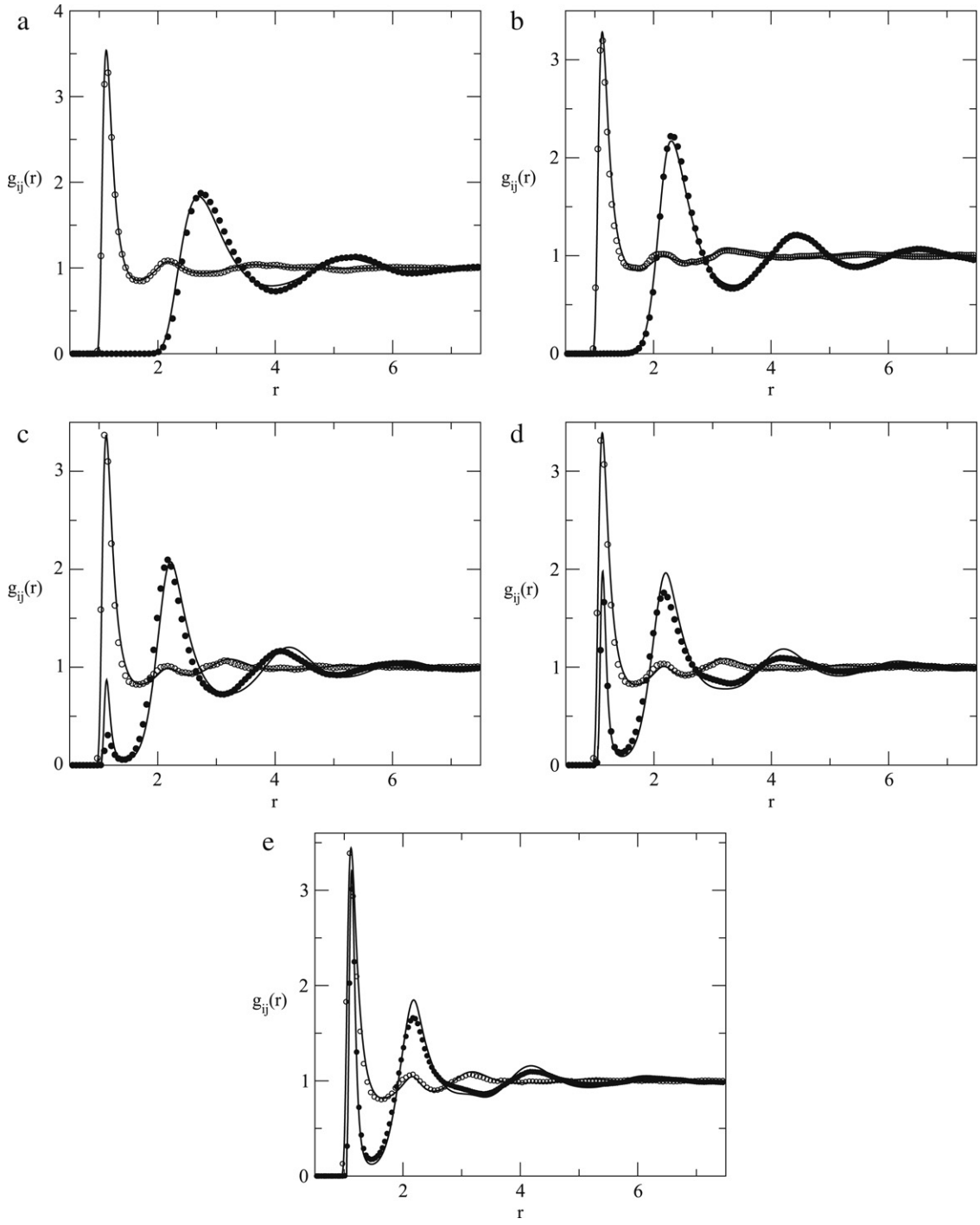

Fig. 4. A comparison of the fluid–matrix and fluid–fluid pair distribution functions from the ROZ/HNC approximation (solid lines) and GCMC simulation data (hollow circles — fluid–matrix, filled circles — fluid–fluid) for the system at $\rho_m^* = 0.3$, $T_m^* = 1.5$, at $T_f^* = 0.1$. Parts a, b, c, d and e correspond to $\mu^* = 0.2$, $\mu^* = 4.2$, $\mu^* = 7.7$, $\mu^* = 10.4$ and $\mu^* = 14.4$, respectively. The adsorbed fluid densities are: 0.05, 0.092, 0.125, 0.155 and 0.204, respectively.

on density and on chemical potential at $T_f^* = 0.2$ is given in Fig. 6. It can be seen that the anomalous behavior of the diffusion coefficient is closely related to what we have observed for heat capacity. Namely, the region of fluid density in which the diffusion coefficient anomaly is observed shrinks with increasing matrix density. At $\rho_m^* = 0.2$, the anomaly is well pronounced. At even higher matrix density, $\rho_m^* = 0.3$ the diffusion coefficient is so low that it is difficult to judge if the anomaly still persists. However, equilibrium between a fluid in different matrices and in the bulk occurs at the same value for the chemical potential, Fig. 6b. There we observe that the maxima and minima of the diffusion coefficient shift to

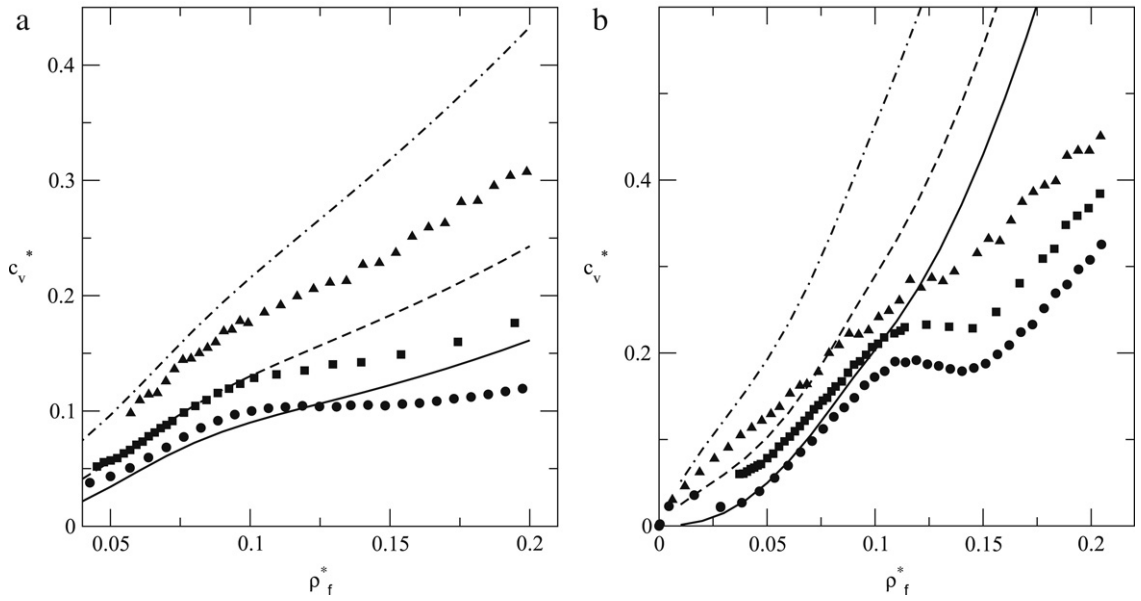

Fig. 5. A comparison of the reduced heat capacity of the core-softened fluid in the bulk and adsorbed in matrices of different densities at $T_m^* = 1.5$ from the GCMC simulation (symbols) and ROZ/HNC theory (lines). Part a: The circles, squares and triangles are for the bulk fluid and in the matrix at $\rho_m^* = 0.1$ and $\rho_m^* = 0.3$, respectively. The corresponding solid, dashed and dash-dotted lines are for the same conditions. In all the three cases $T_f^* = 0.5$. Part b: The same as in part a but at $T_f^* = 0.2$.

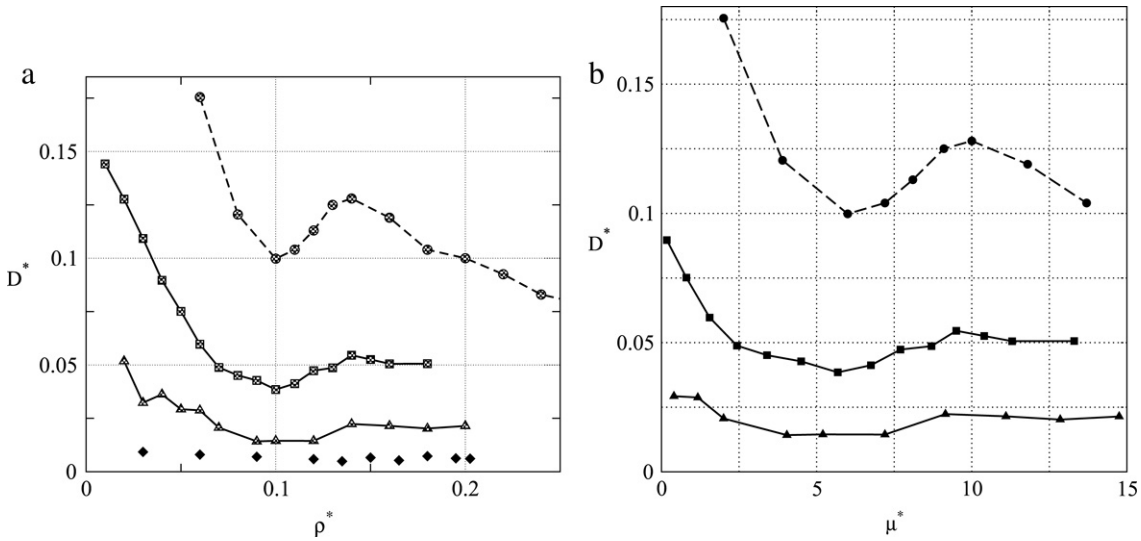

Fig. 6. The dependence of the diffusion coefficient of core-softened fluid on density (part a) and on chemical potential (part b) $T_f^* = 0.2$. The lines with circles, squares, triangles and diamond points correspond to the bulk fluid, the fluid confined in the matrix at $\rho_m^* = 0.1$ and $\rho_m^* = 0.2$, and $\rho_m^* = 0.3$ (only in part a), respectively.

lower values of the chemical potential in denser matrices comparing to the bulk. The anomalous behavior of the diffusion coefficient depresses simultaneously. The disappearance of the diffusion anomaly in dense matrices can be attributed to a low fraction of volume available for adsorption and to the way how fluid density changes upon increasing chemical potential. It is evident that the structural changes as a background for diffusion anomaly cannot be realized under strong confinement in the manner similar to the bulk fluid or if the fraction of volume available for adsorption is high (dilute matrices).

To conclude, we have attempted to describe the structure and thermodynamics of a fluid phase for the core-softened fluid model in disordered matrices by using grand canonical Monte Carlo simulations. In addition, some theoretical results are obtained from the replica Ornstein–Zernike integral equations with the hypernetted chain closure. The adsorption isotherms, the pair distribution functions, the heat capacity are discussed in great detail. We observe that the pair distribution functions for the model confined in different matrices change with increasing fluid density in the manner similar

to the bulk fluid. However, we were unable to introduce a quantitative measure for the structural anomaly, in contrast to the bulk model where such a measure can describe anomalous behavior of the microscopic structure. On the other hand, we have observed that the adsorption isotherm at low temperature exhibits peculiarity in close similarity to the bulk model. In general, theoretical predictions are in reasonable agreement with computer simulation data for adsorption isotherms and pair distribution functions. However, the ROZ/HNC approach fails to describe the microscopic structure well in the region of densities between $\rho_f^* \simeq 0.11$ and 0.17, in this density interval one expects that thermodynamic anomalies occur.

Confirmation of anomalous behavior one can find in the data for heat capacity of the model, in the bulk and under confinement in disordered matrices. Computer simulation data show that the anomalous behavior of heat capacity shrinks with increasing matrix density if adsorption is performed at low temperature. At high temperatures such an anomaly disappears. The present theoretical approach does not describe trends of behavior of heat capacity except at low fluid densities. It seems that the reason is not only lies in the description of changes of microscopic structure at small interparticle separations (here we have seen that the distribution functions from ROZ/HNC approach are satisfactory in the majority of cases) with temperature. Rather the inaccuracies at intermediate separations and specifically of the fluid–fluid correlations in a certain window of thermodynamic states contribute to the failure of the theory to describe the heat capacity data. We have attempted to use the Percus–Yevick approximation but seen that it is unsatisfactory as well. Thus, one must consider application of more sophisticated thermodynamically consistent closures to integral equations at hand, at least there is enough room for improvement in this aspect.

Finally, we have presented data for the dependence of the diffusion coefficient of the model under confinement to show that the anomalous behavior becomes depressed and eventually disappears in dense matrices. However, the anomaly manifested in the growth of the diffusion coefficient with increasing density is observed approximately in the interval of density 0.10–0.14 that coincides with the interval for the peculiar behavior of heat capacity. In our opinion, the accumulated computer simulation data are useful on their own and one can attempt investigation of the fluid model in matrices prepared via special algorithms, like diffusion limited or reaction limited cluster aggregation in future studies. However, it seems more important and urgent to develop and test new theoretical approaches as we have mentioned above. Moreover, it is important to apply computer simulations and theory to describe a set of models with soft-core repulsion and/or repulsive harsh shoulder with stronger attraction to get knowledge about the interplay of structural, thermodynamic and dynamic anomalies on the one hand and liquid–vapor and liquid–liquid phase transitions on the other, see e.g. recent works [49,50] for the description of some aspects of this challenging issue.

Acknowledgements

This project has been partially supported by the CONACyT of Mexico and the Hungarian Academy of Sciences under international collaboration grant as well as by the National University of Mexico under grant IN-223808-2.

References

[1] L.D. Gelb, K.E. Gubbins, R. Radhakrishnan, M. Sliwińska-Bartkowiak, Rep. Prog. Phys. 62 (1999) 1573.
[2] M. Schoen, Computer Simulations of Condensed Phases in Complex Geometries, Springer, Berlin, Heidelberg, 1993.
[3] M Schoen, in: M. Borówko (Ed.), Computational Methods in Surface and Colloid Science, Dekker, New York, 2000, Chapter 1.
[4] M.-C. Bellissent-Funel, J. Phys.: Condens. Matter 13 (2001) 9165.
[5] V. Crupi, D. Majolino, P. Migliardo, V. Venuti, M.-C. Bellissent-Funel, Mol. Phys. 101 (2003) 3323.
[6] N. Floquet, J.P. Coulomb, N. Dufau, G. Andre, R. Kahn, Adsorption 11 (2005) 139.
[7] P. Gallo, M. Rovere, E. Spohr, J. Chem. Phys. 113 (2000) 11324.
[8] M. Jorge, N.A. Seaton, Mol. Phys. 100 (2002) 2017.
[9] J. Marti, G. Nagy, M.C. Gordillo, E. Guárdia, J. Chem. Phys. 124 (2006) art. 094703.
[10] P. Setny, M. Geller, J. Chem. Phys. 125 (2006) art. 144717.
[11] J. Wu, AIChE J. 52 (2005) 1169.
[12] W.G. Madden, E.D. Glandt, J. Stat. Phys. 51 (1988) 537.
[13] J. Given, G. Stell, Physica A 209 (1994) 495.
[14] M.L. Rosinberg, in: C. Caccamo, J.P. Hansen, G. Stell (Eds.), New Approaches to Problems in Liquid State Theory, Kluwer Academic Publ, Dordrecht, 1999, p. 245.
[15] O. Pizio, in: M. Borówko (Ed.), Computational Methods in Surface and Colloid Science, Marcel Dekker, New York, 2000, Chapter 6.
[16] M. Schmidt, J. Phys.: Condens. Matter 17 (2005) S3481.
[17] M. Alvarez, D. Levesque, J.J. Weis, Phys. Rev. E 60 (1999) 5495.
[18] R.J. Pellenq, S. Rodts, V. Pasquier, A. Delville, P. Levitz, Adsorption 6 (2000) 241.
[19] J.K. Brennan, W. Dong, J. Chem. Phys. 116 (2002) 8948.
[20] X. Yanga, X. Yue, Colloids and Surfaces A 301 (2007) 166.
[21] E. Lomba, J.A. Given, G. Stell, J.J. Weis, D. Levesque, Phys. Rev. E 48 (1993) 233.
[22] R.D. Kaminsky, P.A. Monson, J. Chem. Phys. 95 (1991) 2936.
[23] C. Vega, R.D. Kaminsky, P.A. Monson, J. Chem. Phys. 99 (1993) 3003.
[24] K.S. Page, P.A. Monson, Phys. Rev. E 54 (1996) R29.
[25] P. Gallo, M. Rovere, Phys. Rev. E 76 (2007) art. 061202.
[26] L. Sarkisov, P.R. van Tassel, J. Phys.: Condens. Matter 20 (2008) 333101.
[27] F.X. Prielmeier, E.W. Lang, R.J. Speedy, H.D. Ludermann, Phys. Rev. Lett. 59 (1987) 1128.
[28] F. Sciortino, A. Geiger, H.E. Stanley, Nature (London) 354 (1991) 218.
[29] J.R. Errington, P.G. Debenedetti, Nature (London) 409 (2001) 318.
[30] P.G. Debenedetti, J. Phys.: Condens. Matter 15 (2003) R1669.
[31] G. Franzese, K. Stokely, X.-Q. Chu, P. Kumar, M.G. Mazza, S.-H. Chen, H.E. Stanley, J. Phys.: Condens. Matter 20 (2008) 494210.
[32] C.A. Angell, R.D. Bressel, M. Hemmatti, E.J. Sare, J.C. Tucker, Phys. Chem. Chem. Phys. 2 (2000) 1559.

[33] M.S. Shell, P.G. Debenedetti, A.Z. Panagiotopoulos, Phys. Rev. E 66 (2002) art. 011202.
[34] P.A. Netz, F.W. Starr, H.E. Stanley, M.C. Barbosa, J. Chem. Phys. 115 (2001) 344.
[35] E.A. Jagla, J. Chem. Phys. 111 (1999) 8980.
[36] G. Franzese, G. Malescio, A. Skibinsky, S.V. Buldyrev, H.E. Stanley, Nature (London) 409 (2001) 692.
[37] A. Barros de Oliveira, P.A. Netz, T. Colla, M.C. Barbosa, J. Chem. Phys. 124 (2006) art. 084505.
[38] A. Barros de Oliveira, P.A. Netz, T. Colla, M.C. Barbosa, J. Chem. Phys. 125 (2006) art. 124503.
[39] A. Barros de Oliveira, G. Franzese, P.A. Netz, J. Chem. Phys. 128 (2008) art. 064901.
[40] H. Dominguez, O. Pizio, L. Pusztai, S. Sokołowski, Ads. Sci. and Technology 25 (2007) 479.
[41] M. Allen, D. Tildesley, Computer Simulation of Liquids, Clarendon, Oxford, 1987.
[42] A. Meroni, D. Levesque, J.J. Weis, J. Chem. Phys. 105 (1996) 1101.
[43] A. Trokhymchuk, O. Pizio, M. Holovko, S. Sokołowski, J. Chem. Phys. 106 (1997) 200.
[44] E. Kierlik, M.L. Rosinberg, G. Tarjus, P.A. Monson, J. Chem. Phys. 106 (1997) 264.
[45] B. Hribar, V. Vlachy, O. Pizio, Molec. Phys. 100 (2002) 3093.
[46] G. Sarkisov, E. Lomba, J. Chem. Phys. 122 (2005) art. 214504.
[47] O. Pizio, H. Dominguez, Yu. Duda, S. Sokołowski, J. Chem. Phys. (in press).
[48] W.P. Krekelberg, J. Mittal, V. Ganesan, T.M. Truskett, Phys. Rev. E 77 (2008) art. 041201.
[49] G. Franzese, J. Molec. Liq. 136 (2007) 267.
[50] W. R zysko, O. Pizio, A. Patrykiejew, S. Sokołowski, J. Chem. Phys. 129 (2008) art. 124502.